Journal of Catalysis 282 (2011) 237–247

Contents lists available at ScienceDirect

Journal of Catalysis

journal homepage: www.elsevier.com/locate/jcat

Liquid-phase glycerol hydrogenolysis to 1,2-propanediol under nitrogen pressure using 2-propanol as hydrogen source

I. Gandarias *, P.L. Arias, J. Requies, M. El Doukkali, M.B. Güemez

School of Engineering (UPV/EHU), Calle Alameda Urquijo s/n, 48013 Bilbao, Spain

ARTICLE INFO

Article history:
Received 16 February 2011
Revised 26 May 2011
Accepted 17 June 2011
Available online 26 July 2011

Keywords:
Glycerol
Hydrogenolysis
Propanediol
Catalytic transfer hydrogenation
Ni–Cu/Al_2O_3
Hydride

ABSTRACT

2-Propanol was studied as a hydrogen donor molecule in the transfer hydrogenation process to selectively convert glycerol into 1,2-propanediol under N_2 pressure and using Ni or/and Cu supported on Al_2O_3 catalysts. The results were compared to those obtained under the same operating conditions but under H_2 pressure. The results of the activity tests and catalyst characterization techniques (N_2-physisorption, H_2-chemisorption, TPD of NH_3, TPR, TPO and XPS) suggest that glycerol hydrogenolysis to yield 1,2-propanediol occurred through a different mechanism regarding the origin of the hydrogen species. When atomic hydrogen came from dissolved molecular hydrogen dissociation, glycerol was first dehydrated to acetol and then hydrogenated to 1,2-propanediol. On the other hand, when the hydrogen atoms were produced from 2-propanol dehydrogenation, glycerol was directly converted to 1,2-propanediol through intermediate alkoxide formation.

1. Introduction

Nowadays, there is a tendency to reduce the use of fossil hydrocarbon sources in the production of commodity chemicals. The main reasons are increasing and fluctuating oil prices, the drive to renewable resources and a global concern to reduce CO_2 emissions. Glycerol, obtained as a by-product in biodiesel manufacture, is a versatile feedstock for the production of a whole range of chemicals, polymers and fuels [1]. The glycerol hydrogenolysis process for obtaining propanediols (PDOs) has aroused considerable interest due to the attractive applications of 1,2-PDO, an important commodity chemical traditionally derived from propylene oxide, and 1,3-PDO, a monomer that can be used to produce polyester fibres. In the reaction pathway, glycerol is first dehydrated to 1-hydroxypropan-2-one (acetol) or 3-hydroxypropanal (3-HPA), which are subsequently hydrogenated to 1,2 and 1,3-PDO, respectively [2]. Several reaction systems have been studied to maximize glycerol conversion and PDO selectivity. Dasari et al. developed a two-step reaction process using a copper chromite catalyst. In the first step, acetol was produced through glycerol reactive distillation at 473 K and 0.65 bar, while in the second step the acetol was further hydrogenated to 1,2 PDO at 473 K and 13.8 bar hydrogen pressure [3]. Interesting results have been reported using Cu/Al_2O_3 in single-step vapour-phase glycerol hydrogenolysis at near ambient hydrogen pressure [4,5]. Liquid-phase glycerol hydrogenolysis has also been studied [6–10], as it has both energy- and plant-scale reduction benefits. Nevertheless, reported results are not as promising as the ones from vapour phase and two-step processes. In liquid-phase reactions, high hydrogen pressures are needed due to the low solubility of hydrogen in glycerol/water solutions, and limited H_2 availability may cause undesired side reactions such as cracking and coking.

Hydrogen accessibility problems could be avoided if the hydrogen required for glycerol hydrogenolysis was to be generated directly in the active sites of the catalyst, allowing a process with inert atmosphere and lower working pressure. Among others, two different processes can be considered to generate hydrogen: aqueous-phase reforming (APR) and catalytic transfer hydrogenation (CTH). Hydrogen production from glycerol APR is a well-reported process [11,12].

$$C_3H_5(OH)_3 + 3H_2O \rightarrow 3CO_2 + 7H_2$$

The production of PDOs by APR of glycerol has already been studied [13]. The process initially involves hydrogen and CO_2 formation. The hydrogen produced in the reforming step is then consumed in the hydrogenolysis of glycerol, leading to an overall conversion of glycerol to 1,2-PDO, CO_2 and water [14].

CTH, in which hydrogen is transferred from a hydrogen donor molecule to an acceptor, is an interesting process for reducing organic compounds, as it has real advantages compared to processes with molecular hydrogen. Molecular hydrogen has high diffusibility, being easily ignited and presents considerable hazards on a large

* Corresponding author. Address: Escuela Técnica Superior de Ingeniería, Alameda Urquijo s/n, PC 48013 Bilbao, Spain. Fax: +34 946 014 179.
E-mail address: inaki_gandarias@ehu.es (I. Gandarias).

0021-9517/$ - see front matter © 2011 Elsevier Inc. All rights reserved.
doi:10.1016/j.jcat.2011.06.020

scale; the use of hydrogen donors obviates these difficulties [15]. Alcohols have been widely used in CTH processes [16], and 2-propanol is a suitable hydrogen donor for glycerol hydrogenolysis [17].

This paper studies aqueous-phase reforming and catalytic transfer hydrogenation processes as sources of hydrogen for glycerol hydrogenolysis to PDOs.

2. Experimental

2.1. Catalysts

Amorphous silica-alumina loaded with 1 wt.% Pt (Pt/ASA) was kindly supplied by Shell, while Ni—Cu/$Al_2O_3^{(A)}$ was kindly supplied by the Boreskov Institute of Catalysis. $CuCr_2O_3$ was purchased from Süd-Chemie. Ni/$Al_2O_3^{(S)}$, Cu/$Al_2O_3^{(S)}$ and Ni—Cu/$Al_2O_3^{(S)}$ were prepared by the sol–gel method. Aluminium isopropoxide (Aldrich) was dissolved in deionised water (9 mL of H_2O per gram of aluminium isopropoxide) by vigorous stirring of the solution at 313 K. The pH was measured and kept between 3.8 and 4.2 adding the required amounts of HNO_3 (0.5 M). Simultaneously, nickel(II) nitrate hexahydrate (Aldrich) and/or Copper(II) nitrate hemi pentahydrate (Alfa Aesar) were dissolved in ethanol. The precursor solution was slowly added to an aluminium isopropoxide solution. The mixture was stirred for 30 min at 313 K and then introduced into the ultrasonic apparatus for another 30 min. The mixture was then rested for 24 h at 313 K and subsequently for another 12 h at 375 K. The product obtained was crushed and calcined from room temperature to 723 K at a heating rate of 2 K/min. The temperature was maintained for 4 h. Catalyst samples for activity tests were used in powdered form with a granule size between 320 and 500 μm.

2.2. Activity test

The hydrogenolysis of glycerol was carried out in a 50 mL stainless steel autoclave with a magnetic stirrer. The catalyst powder (166 mg catalyst/g of glycerol) was introduced into the autoclave and the reactor was then purged with H_2 or N_2. After purging, some of the catalysts (Ni—Cu/$Al_2O_3^{(A)}$, Ni—Cu/$Al_2O_3^{(S)}$, Ni/$Al_2O_3^{(S)}$ and Cu/$Al_2O_3^{(S)}$) were pre-treated, reducing them under a 50 vol.% H_2/N_2 flow for 4 h at 593 or 723 K, while the others (Pt/ASA and $CuCr_2O_3$) were used as received. Next, the reactor temperature was set to 493 K and the N_2 or H_2 pressure was increased to 45 bar. The aqueous solution (41 mL) with the reactants was placed on a feed cylinder and heated to the reaction temperature. The reaction starting time was established when the line connecting the feed cylinder and the reactor was opened. During the reaction, changes in the system pressure were observed: a decrease in the experiments under H_2 pressure (due to H_2 consumption), and an increase in the experiments under N_2 pressure when a hydrogen donor molecule was added (due to the formation of H_2 and other gaseous species). Nevertheless, as diluted glycerol and donor feeds were used, the pressure variations were negligible.

Five liquid samples were taken throughout the reaction in order to obtain the time evolution of reactant and product concentrations. These compounds were analysed using a gas chromatograph (Agilent Technologies, 7890 A) equipped with a flame ionization detector (FID) and a thermal conductivity detector (TCD). A Meta-Wax capillary column (diameter 0.53 mm, length 30 m) was used for product separation. After reaction, the gas phase was collected in a gas bag and analysed with another GC-TCD-FID (Agilent Technologies, 7890 A) equipped with a molecular sieve column (HP-MOLESIEVE, diameter 0.535 mm, length 30 m) and a capillary column (HP-PLOT/Q, diameter 0.320 mm, length 30 m). The conversion of the reactants was calculated according to following equation:

$$\text{Conversion of glycerol. } \% = \frac{\text{sum of C-based mol of all liquid prod. } t = t}{\text{C-based mol of glycerol. } t = 0}$$

The selectivity of the products was calculated on a carbon basis.

$$\text{Selectivity of liquid products } \% = \frac{\text{C-based mol of the product}}{\text{Sum of C-based mol of all liquid products}}$$

Initial Turnover Number (TON_0) was calculated as the ratio between the converted amount of glycerol in the first 2 h per gram of catalyst and per hour.

2.3. Catalyst characterization

The catalysts were chemically analysed by Inductively Coupled Plasma Atomic Emission (ICP-AES) using a Perkin–Elmer Optima 2000 instrument. The solid samples were first digested with a mixture of HF, HCl and HNO_3 at 453 K in a microwave oven. Surface area, pore volume and pore size distributions were determined with N_2 physisorption at 77 K on a Quantachrome AUTOSORB-1C instrument. Prior to the analysis, all samples were dried at 393 K overnight under high vacuum. The surface area was calculated using the Brunauer, Emmett and Teller (BET) method, while pore size distributions were calculated using the Barrett–Joyner–Halenda (BJH) method applied to the desorption leg of the isotherms.

The reducibility of catalysts was studied by hydrogen temperature-programmed reduction (TPR) on a Quantachrome AUTOSORB-1C apparatus with TPR capability. The catalyst sample was reduced in flowing gas containing 5 vol.% H_2 in Ar at a total flow rate of 50 mL/min, using a heating rate of 10 K/min up to a final temperature of 1223 K. A TCD detector downstream of the sample monitored changes in the concentration of H_2. Hydrogen chemisorption was performed at 313 K with the Quantachrome AUTOSORB-1C volumetric system. All the catalysts were reduced at 873 K in pure H_2 flow for 4 h prior to the measurements. The quantity of H_2 adsorbed at monolayer coverage was estimated by extrapolating the linear portion of the isotherms to zero pressure.

Temperature-programmed oxidation analyses of fresh and used catalysts were carried out using a thermo-gravimetric analyser (Mettler Toledo TGA/SDTA 851e). The standard protocol involved the pre-treatment of the sample (45–50 mg) in 125 mL/min of N_2 flow from 297 K to 673 K at a heating rate of 10 K/min. The sample was then cooled to 323 K and the weight change of the sample was continuously monitored during its heating in 125 mL/min of N_2 as purge gas and 75 mL/min of 10 vol.% O_2 in He as reactive gas from 323 to 1173 K at a heating rate of 5 K/min.

The acidity of the freshly reduced samples was determined by ammonia temperature-programmed desorption (TPD) measurements. The sample was pre-treated in a He stream at 673 K for 0.5 h and then cooled to 373 K and ammonia-saturated using a stream of 5 vol.% NH_3/He flow (50 mL/min) for 0.5 h. Following catalyst equilibration in a helium flow, the ammonia was desorbed using a linear heating rate of 10 K/min to 723 K. The area under the curve was integrated to determine the total acidity of the sample from its NH_3 desorption profile.

X-ray photoelectron spectroscopy (XPS) studies were performed with a Physical Electronics PHI 5700 spectrometer equipped with a hemispherical electron analyser (model 80-365B) and a Mg Kα (1253.6 eV) X-ray source. High-resolution spectra were recorded at a 45° take-off-angle by a concentric hemispherical analyser operating in the constant pass energy mode at 29.35 eV, using a 720 mm diameter analysis area. Charge referencing was done against adventitious carbon (C 1s 284.8 eV). The pressure in the analysis chamber was kept below 5×10^{-6} Pa. The PHI

ACCESS ESCA-V6.0 F software package was used for data acquisition and analysis. A Shirley-type background was subtracted from the signals. Recorded spectra were always fitted using Gauss–Lorentz curves in order to more accurately determine the binding energy of the different element core levels.

3. Results and discussion

3.1. Hydrogen donor selection

In order for cross-oxidation/reduction to occur, it has been reported that adjacent sites may be necessary for donor and acceptor [18]. Therefore, the first criterion to be fulfilled by the selected hydrogen donor molecules was to be soluble in glycerol. Moreover, in order to improve the process yield, reactions other than dehydrogenation of the donor should be minimized under the operating conditions.

Alcohols have shown to be suitable for the CTH of ketones and are soluble in glycerol. Within a series of alcohol isomers, it is reported that 2-alkanols have higher catalytic activity than 3-alkanols [19]. Use was made of 2-propanol (2-PO) as it is soluble in both glycerol and water, and it has already been used as a hydrogen donor molecule in glycerol hydrogenolysis [17]. Under these operating conditions, 2-PO can be dehydrogenated to acetone or dehydrated to propene.

3.2. Initial catalyst screening

The choice of a suitable catalytic system for the hydrogenation processes selected was by no means random, as it had to fulfil several requirements. The glycerol hydrogenolysis process requires a bi-functional catalyst with active sites for glycerol dehydration and active sites for acetol hydrogenation. Interesting results for glycerol hydrogenolysis have been obtained with $CuCr_2O_3$ catalyst [3,5,20]. Ni–Cu-based catalysts have been used for heterogeneous transfer reactions [16]. On the other hand, Pt silica–alumina catalysts have proven to be effective for alkane production by the APR of sorbitol [21]. Taking all these considerations into account, three commercial catalysts were tested: Pt/ASA, Ni—Cu/$Al_2O_3^{(A)}$ and $CuCr_2O_3$.

Three activity tests were arranged for each of the selected catalysts: under H_2 pressure, under N_2 pressure and under N_2 pressure but adding 2-PO as a hydrogen donor molecule (1:1 glycerol/2-PO molar ratio). In the experiments with $CuCr_2O_3$ and Ni—Cu/$Al_2O_3^{(A)}$, C3 products (acetol, 1,2-PDO, 1,3-PDO and 1-propanol) and products resulting from C–C bond cleavage (ethylene glycol, ethanol, methane, and CO_2) were detected. In the experiments using Pt/ASA, and besides those products, methanol, ethane, propanal and propanoic acid were also detected. In the experiments where 2-PO was added as a hydrogen donor molecule, acetone was detected coming from 2-PO dehydrogenation, and propane and propene were observed in the gas phase coming from 2-PO and acetone dehydration.

First, the effect of the hydrogen source will be discussed. Under H_2 pressure, most of the acetol formed from glycerol dehydration was hydrogenated to 1,2-PDO (see Fig. 1A), showing that under a 45 bar H_2 atmosphere, the hydrogenation of acetol was effective with all three catalysts and that the controlling step in this hydrogenolysis process under H_2 pressure seems to be the glycerol dehydration step. In the experiments under N_2 pressure, part of the acetol formed from glycerol dehydration was not hydrogenated; nevertheless, higher selectivities to 1,2-PDO were measured with the addition of 2-PO (Fig. 1A). Therefore, it seems that CTH using 2-PO was more effective than glycerol APR for propanediol formation. Moreover, as can be observed in Fig. 1B, the greater glycerol conversion for Pt/ASA and Ni—Cu/$Al_2O_3^{(A)}$ catalysts was achieved in the tests with the hydrogen donor, indicating that generating hydrogen directly in the active sites benefits glycerol conversion.

Concerning the effect of the catalyst, it can be observed that Cu-Cr_2O_3 catalyst had extremely low activity under all the operating conditions tested. In the case of Pt/ASA, lower selectivities to the first hydrogenolysis products (acetol + 1,2-PDO) were observed as compared to Ni—Cu/$Al_2O_3^{(A)}$. It is well known that Pt combined with strong acid sites catalyses the C–C bond cleavage [11]; therefore, cracking product formation and further 1,2-PDO hydrogenolysis to 1-propanol were responsible for the lower selectivity values to the initial hydrogenolysis products obtained with Pt/ASA. Cu-Cr_2O_3 catalyst did not effectively dehydrogenate 2-PO (low 2-PO conversion and low selectivity to acetone). Pt and Ni–Cu metal sites were more effective in 2-PO dehydrogenation and therefore in the CTH process.

In the light of these results, the use of a hydrogen donor seems to be a more effective source of hydrogen for glycerol hydrogenolysis than glycerol APR. It was therefore decided to prepare three catalysts by the sol–gel method: Cu/$Al_2O_3^{(S)}$, Ni—Cu/$Al_2O_3^{(S)}$ and Ni/$Al_2O_3^{(S)}$ in order to perform a more thorough study of glycerol hydrogenolysis by CTH.

3.3. Glycerol hydrogenolysis by CTH on Ni and/or Cu Al_2O_3

3.3.1. N_2 physisorption and metal dispersion

Table 1 summarises the metal content together with the main textural properties of the calcined catalysts and the chemisorption analysis results. All samples presented Type IV isotherms with the hysteresis loops typical of mesoporous materials. The lower surface area of the impregnated samples with respect to bare $Al_2O_3^{(S)}$ (also prepared by sol–gel) is consistent with the relative high metal loading (7–35%). Ni—Cu/$Al_2O_3^{(S)}$ and Cu/$Al_2O_3^{(S)}$ had similar metal loadings; however, the measured Ni—Cu/$Al_2O3^{(S)}$ surface area and cumulative pore volume were significantly higher as compared to Cu/$Al_2O_3^{(S)}$. As observed in Table 1, the metal dispersion values obtained from hydrogen chemisorption analysis follow the order: Ni > Ni–Cu > Cu. This trend suggests that Cu particles are significantly bigger than Ni and Ni–Cu particles. Therefore, big Cu particles could block the pores of the Al_2O_3 structure, reducing the surface accessible for N_2 adsorption.

3.3.2. Temperature-programmed reduction

The TPR spectra of the investigated samples are shown in Fig. 2. Calcined Ni/$Al_2O_3^{(S)}$ recorded one reduction peak at 650 K and another broad peak reduction profile in the 820–1200 K temperature range. This fact suggests the presence of a mixture of NiO_x species due to the different interaction of NiO particles with the support [22]. On Ni-based catalysts, the low-temperature H_2 uptakes are attributed to the reduction of NiO particles weakly interacting with the support, while the high temperature ones are assigned to the reduction of NiO species in close contact with the support or forming species such as $NiAl_2O_4$ [23]. The XPS analysis (discussed later) of Ni/$Al_2O_3^{(S)}$ and Ni—Cu/$Al_2O_3^{(S)}$ samples proved the presence of $NiAl_2O_4$ in the surface of the catalyst. Calcined Cu/$Al_2O_3^{(S)}$ recorded two reduction peaks at 580 and 690 K. The reduction of CuO to Cu^0 generally proceeds in one step, so the peaks at 580 and 690 K could be attributed to the reduction of two different oxidized copper species. Previous works noted the presence of two reduction peaks for Cu/zeolite supported catalysts [24,25]. It is suggested that the lower peak corresponds to the reduction of CuO crystallites and the higher one to the reduction of Cu^{2+} fixed to the support. A comparison of the TPR profile of Ni—Cu/$Al_2O_3^{(S)}$ with the profile of Ni/$Al_2O_3^{(S)}$ reveals that the former records a displacement to lower

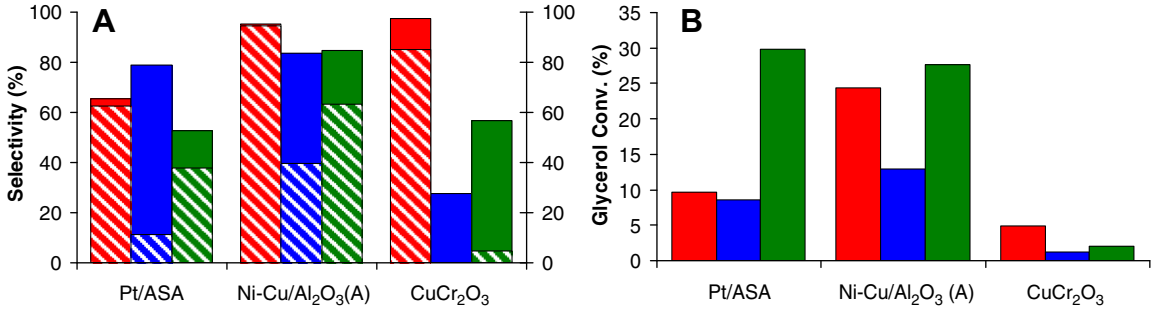

Fig. 1. Selectivity values (A) to first hydrogenolysis products: 1,2-PDO (stripes) and acetol (plain), and glycerol conversion values (B) as a function of the catalyst used and the reaction atmosphere: H_2 atmosphere. N_2 atmosphere. N_2 atmosphere + 2-PO (1:1 glycerol:2-PO molar ratio) 24-h reaction time, 45 bar pressure, 493 K, 41 mL (4 wt.%) glycerol aqueous solution, 166 mg catalyst/g glycerol.

Table 1
Characteristics of the catalysts.

Sample	Ni[a] (wt.%)	Cu[a] (wt.%)	SBET[b] (m^2/g Al_2O_3)	Total pore volume (mL/g)	Dispersion (%)	MSA[c] (m^2/g)	Crystallite size[d] (nm)
$Cu/Al_2O_3^{(S)}$	–	31.7	161	0.12	0.9	1.9	112
$Ni—Cu/Al_2O_3^{(S)}$	7.7	28.0	208	0.16	1.6	3.7	65.6
$Ni/Al_2O_3^{(S)}$	6.9	–	262	0.23	7.4	3.4	13.7
$Al_2O_3^{(S)}$	–	–	298	0.21	–	–	–

[a] Chemical composition determined with ICP.
[b] BET surface area.
[c] Metal Surface Area.
[d] Assuming spherical geometry and H_2:M = 2:1 stoichiometry.

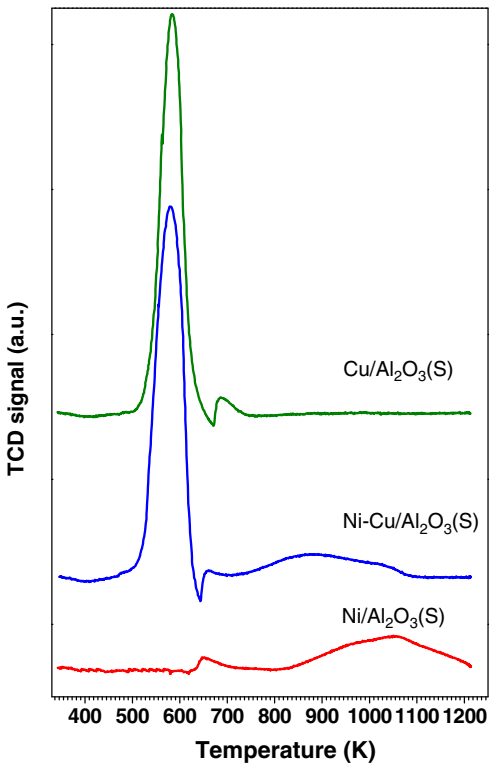

Fig. 2. TPR profiles of calcined $Cu/Al_2O_3^{(S)}$, $Ni-Cu/Al_2O_3^{(S)}$ and $Ni/Al_2O_3^{(S)}$.

temperatures of the peak related to NiO in close contact with the support. It seems that the addition of Cu reduces the interaction between NiO and the support. Hence, the bimetallic system had two reduction peaks at 580 and 660 K related to the reduction of CuO and Cu^{2+} fixed to the support, and a broad peak in the range 720–1050 K that can be associated with the reduction of Ni-based species promoted by the presence of Cu [26].

3.3.3. Temperature-programmed oxidation

The left-hand column in Fig. 3 shows the results for the temperature-programmed oxidation of the three freshly reduced samples. As can be observed, both $Cu/Al_2O_3^{(S)}$ and $Ni—Cu/Al_2O_3^{(S)}$ samples underwent oxidation within the 400–730 K temperature range. However, no weight increments were detected for the $Ni/Al_2O_3^{(S)}$ sample during TPO, suggesting that the reduction treatment applied at 723 K did not lead to any significant reduction of Ni species. This result is consistent with the TPR profile shown previously. The three samples lost weight in the high-temperature range ($T > 700$ K), which might be related to the decomposition of the nitrates remaining in the catalyst after calcination at 723 K [27]. Concerning $Cu/Al_2O_3^{(S)}$ freshly reduced samples, the derivative profile presents two main oxidation peaks at 480 and 643 K, and a smaller one at 730 K. Li and Inui [28] also observed two oxidation peaks in the TPO profiles of reduced $Cu/Zn/Al_2O_3$, which were attributed to the stepwise oxidation of Cu^0. The low-temperature peak, located in the 423–473 K region, was attributed to the oxidation of Cu^0 to Cu^+ and the high-temperature peak (523–573 K) to the oxidation of Cu^+ to Cu^{2+}. In agreement with this study [28], the two main peaks of $Cu/Al_2O_3^{(S)}$ catalyst can be ascribed to the stepwise oxidation of Cu^0. In this work, the peaks are shifted towards higher temperatures, indicating a larger copper particle size [29]. Finally, the highest temperature oxidation peak can be attributed to the oxidation of the copper species interacting strongly with the support; the presence of two types of copper species was already observed in the TPR profile previously discussed. For the reduced fresh $Ni—Cu/Al_2O_3^{(S)}$ catalyst, the same three Cu oxidation peaks are observed, but shifted to lower temperatures. As observed in H_2 chemisorption analysis, and also in the XPS analysis discussed below, it seems that the presence of Ni improves copper dispersion, and Cu^0 is therefore oxidized at lower temperatures.

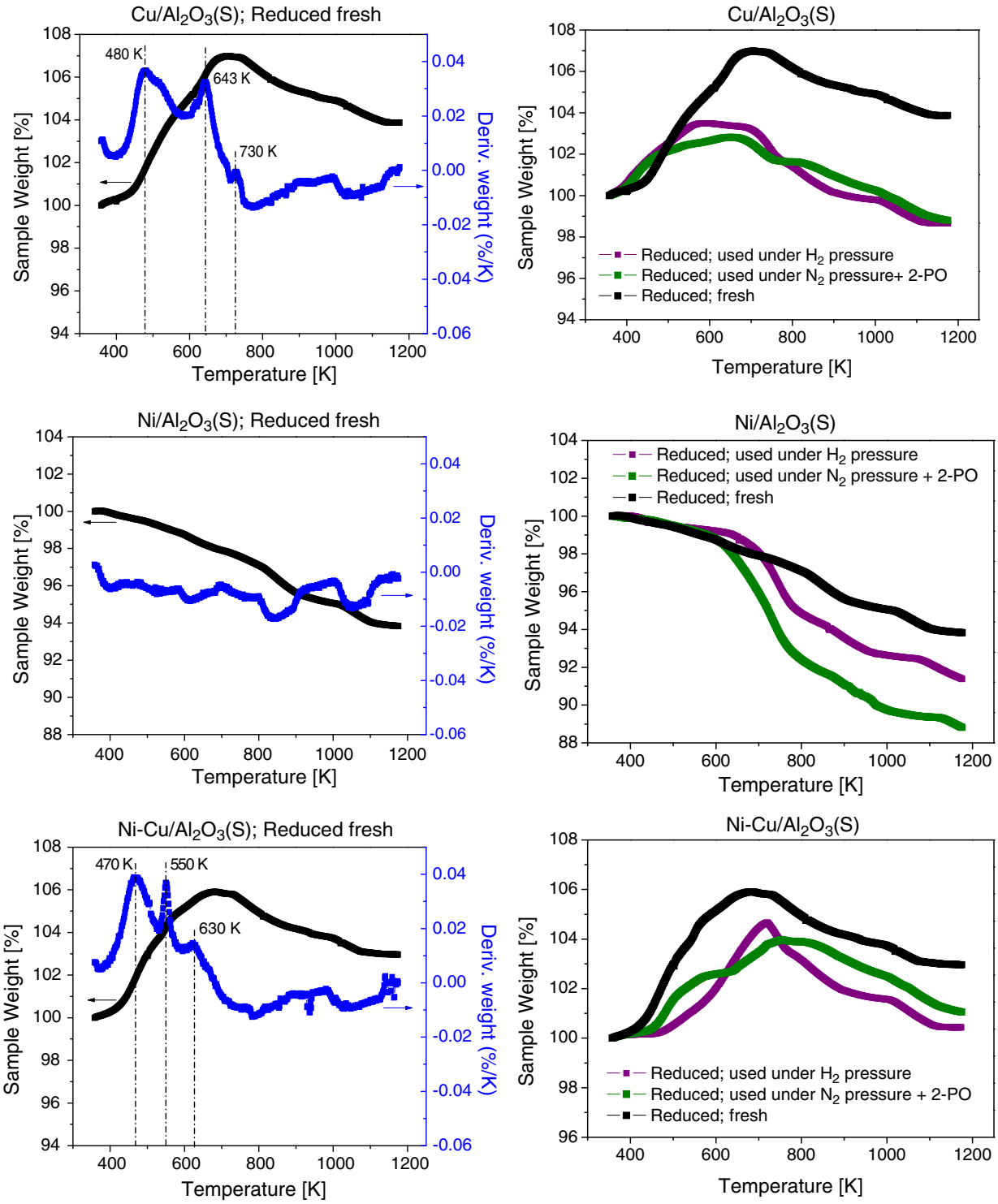

Fig. 3. TGA corresponding to the TPO of reduced fresh samples (left-hand column). Weight change profile of fresh samples and samples used under H_2 or N_2 pressure with 2-PO (right-hand column).

As the thermogravimetric equipment used was not coupled to mass spectrometry, it was not possible to quantify the exact amount of coke formed in the spent samples. Nevertheless, it is possible to carry out a qualitative discussion comparing the variation in sample weight between fresh and spent samples after TPO (see Fig. 3, right-hand column). For both $Cu/Al_2O_3^{(S)}$ and $Ni—Cu/Al_2O_3^{(S)}$ spent samples, similar weight variations were measured regardless of whether they were used under H_2 pressure or N_2 pressure and 2-PO. It can therefore be assumed that coke formation for Cu-based catalysts was independent of the reaction atmosphere. In the case of $Ni/Al_2O_3^{(S)}$, coke formation was slightly enhanced in the activity test under N_2 pressure and 2-PO as compared to the test under H_2 pressure.

3.3.4. Temperature-programmed desorption of ammonia

The total acidity of the fresh samples, which was calculated as the integrated area of the NH_3 desorption profile, is shown in Table 2. There is a decrease in the total acidity of the catalyst with

higher metal loading. As is to be expected, metallic components occupy the acid sites [30].

3.3.5. X-ray photoelectron spectra

For each $Cu/Al_2O_3^{(S)}$, $Ni/Al_2O_3^{(S)}$ and $Ni—Cu/Al_2O_3^{(S)}$ catalyst, three samples were analysed by XPS: (i) reduced at 723 K, (ii) reduced at 723 K and used under H_2 atmosphere and (iii) reduced at 723 K and used under N_2 atmosphere with 2-PO as the hydrogen donor molecule. Atomic surface ratios were computed from XPS peak intensities and the results are presented in Table 3. These results are compared with the bulk theoretical ratios, obtained from ICP values for Cu and Ni content and stoichiometrically for O and Al. As can be observed, Ni/Al surface ratios in reduced fresh samples are close to theoretical bulk Ni/Al ratios, while Cu/Al surface ratios in reduced samples are smaller than theoretical bulk ratios, with the ratio being higher in the $Ni—Cu/Al_2O_3^{(S)}$ sample than in the $Cu/Al_2O_3^{(S)}$ sample. These results are in agreement with the metal dispersion data presented above (Ni > Ni–Cu > Cu). Most of the well-dispersed Ni atoms were accessible for X-ray radiation. On the other hand, $Cu/Al_2O_3^{(S)}$ catalyst had low Cu dispersion and therefore comparatively big Cu particles. Those Cu atoms far from the surface of the big particles were not detected in the XPS measurement, leading to a low Cu/Al ratio. The higher Cu/Al ratio measured for $Ni—Cu/Al_2O_3^{(S)}$ catalyst indicates that the addition of Ni enhanced Cu dispersion.

Similar C/Al ratios were measured for the samples run under H_2 or N_2 pressure. It therefore seems that coke formation was unaffected by the gaseous-phase composition under these experimental conditions, as was also observed in the TPO analysis of spent samples. Concerning metal/Al ratios, the Cu/Al and Ni/Al surface ratios for all three catalysts recorded a significant decrease in the samples used in reaction under H_2 or N_2 pressure. Due to the mild operating conditions (493 K), it does not seem plausible that metal particles underwent significant sinterization, and hence the decrease in the metal/Al surface ratio is probably due to coke deposits.

The chemical species found on the catalyst surfaces and their proportions were also evaluated. For spent catalysts, very low peak intensities were measured for Cu and Ni, with a high noise to peak ratio, as the metal particles were covered by coke. It was not therefore possible to make suitable deconvolutions. For this reason, only the binding energies of core electrons of freshly reduced samples are reported in Table 4. The Cu 2p3/2 level of $Cu/Al_2O_3^{(S)}$ and $Ni—Cu/Al_2O_3^{(S)}$ reduced samples had two components, a main peak at 931.7–932.2 and another one at 933.9–934.2 eV, related to Cu^0 and Cu^{2+}, respectively [31,32]. Therefore, almost all the surface CuO was reduced after catalyst activation. Concerning Ni 2p3/2 in $Ni/Al_2O_3^{(S)}$ and $Ni—Cu/Al_2O_3^{(S)}$ reduced samples, three peaks were obtained after the deconvolution at 852.4–852.7, 854.5 and 856.5–856.7 eV. The first peak corresponds to Ni^0, the second one to Ni^{2+} and the peak at the highest binding energy to $NiAl_2O_4$ [33,34]. It should be noted that after the activation of the samples, only 11–13% of the surface Ni oxide was reduced in $Ni/Al_2O_3^{(S)}$ and $Ni—Cu/Al_2O_3^{(S)}$ samples. Taking into account the TPR spectra shown before, it is clear that under the activation conditions used (723 K), it was not possible to reduce the NiO in close contact with the support and the $NiAl_2O_4$.

Table 2
Acidity of the fresh samples from temperature-programmed desorption of ammonia.

Catalyst	Des. $NH_3 \times 10^4$ (mol g^{-1})
$Cu/Al_2O_3^{(S)}$	3.64
$Ni—Cu/Al_2O_3^{(S)}$	3.39
$Ni/Al_2O_3^{(S)}$	3.95

Table 3
Bulk theoretical ratios and surface atomic ratios obtained by XPS in reduced fresh and reduced spent samples.

Sample		O/Al[a]	C/Al	Cu/Al[b]	Ni/Al[b]
$Cu/Al_2O_3^{(S)}$	Bulk theoretical ratios	1.50	–	0.44	–
	Reduced fresh	1.09	0.19	0.08	–
	Used under N_2 pressure + 2-PO	2.15	0.23	0.01	–
	Used under H_2 pressure	2.20	0.39	0.01	–
$Ni/Al_2O_3^{(S)}$	Bulk theoretical ratios	1.50	–	–	0.07
	Reduced fresh	1.76	0.19	–	0.07
	Used under N_2 pressure + 2-PO	1.98	0.34	–	0.01
	Used under H_2 pressure	2.24	0.35	–	0.003
$Ni—Cu/Al_2O_3^{(S)}$	Bulk theoretical ratios	1.50	–	0.42	0.10
	Reduced fresh	1.13	0.22	0.12	0.06
	Used under N_2 pressure + 2-PO	1.13	0.25	0.02	0.006
	Used under H_2 pressure	2.28	0.18	0.01	0.001

[a] Obtained stoichiometrically.
[b] Data obtained from ICP values for Cu and Ni content and stoichiometrically for Al.

3.3.6. Activity test results and mechanistic discussion

Samples of the three catalysts were tested at 493 K reaction temperature under H_2 pressure and under N_2 pressure adding 2-PO as a hydrogen donor molecule, with the 2-PO/glycerol molar ratio being 1 or 1.5. All the samples were pre-treated prior to the test, reducing them under a 50 vol.% H_2/N_2 flow for 4 h at 593 or 723 K. Fig. 4 shows the glycerol conversion values recorded in each activity test. Major increments in glycerol conversion were observed for all three catalysts and the two reaction atmospheres when the catalyst samples were reduced at 723 K. This fact indicates that, under the reaction conditions investigated, the active sites for the glycerol hydrogenolysis process are reduced sites. For the samples activated at 723 K, glycerol conversion values recorded under H_2 atmosphere follow the order NiCu > Ni > Cu – the same trend as the measured MSA of the catalysts (see Table 1) – while under N_2 atmosphere and 2-PO, the order is NiCu > Cu > Ni. The different trend in glycerol conversion regarding the hydrogen source seems to indicate that different mechanisms and/or different active sites might play a role regarding whether glycerol hydrogenolysis is conducted under H_2 pressure or under N_2 pressure adding 2-PO as hydrogen donor. Focusing on the effect of the amount of added hydrogen donor, when the amount of 2-PO was increased by 50%, the conversion of glycerol increased only slightly.

It is interesting to also compare the results obtained with $Ni—Cu/Al_2O_3^{(S)}$ reduced at 593 K (see Table 5) and the results obtained with $Ni—Cu/Al_2O_3^{(A)}$ also reduced at 593 K (see Fig. 1). It can be observed that a higher glycerol conversion was obtained with $Ni—Cu/Al_2O_3^{(S)}$ (31.0% under H_2 pressure and 41.2% under N_2 pressure plus 2-PO) as compared to the ones obtained with $Ni—Cu/Al_2O_3^{(A)}$ (24.4% under H_2 pressure and 27.7% under N_2 pressure). Due to a confidentiality agreement, no characterization information regarding $Ni—Cu/Al_2O_3^{(A)}$ catalyst can be provided.

Table 4
Binding energies (eV) and relative abundance (%) of core electrons of Cu 2p and Ni 2p in reduced fresh samples.

Sample	Cu 2p3/2 (%)	Ni 2p3/2 (%)
$Cu/Al_2O_3^{(S)}$	931.7 (97)	–
	933.9 (3)	
$Ni/Al_2O_3^{(S)}$	–	852.4 (13)
		854.5 (27)
		856.5 (60)
$Ni—Cu/Al_2O_3^{(S)}$	932.2 (90)	852.7 (11)
	934.2 (10)	854.5 (30)
		856.7 (58)

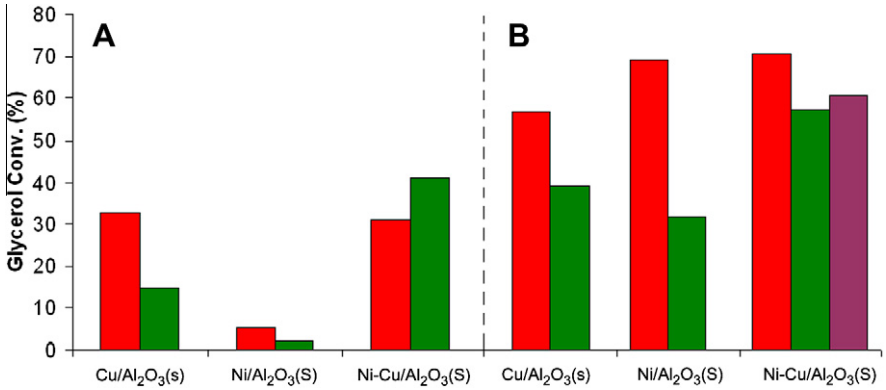

Fig. 4. Glycerol conversion values after 24-h reaction time, 45 bar pressure, 493 K, 41 mL (4 wt.%) glycerol aqueous solution and 166 mg catalyst/g glycerol. (A) 593 K activation temperature, (B) 723 K activation temperature. H_2 atmosphere. N_2 atmosphere + 2-PO (1:1 glycerol:2-PO molar ratio). N_2 atmosphere + 2-PO (1:1.5 glycerol:2-PO molar ratio).

Table 5
Initial Turnover Number (TON_0), and glycerol conversion and selectivity values obtained after 24-h reaction time as a function of the reduction temperature, the catalyst utilized and the reacting atmosphere. 45 bar pressure, 493 K, 41 mL (4 wt.%) glycerol aqueous solution, 166 mg catalyst/g glycerol.

Sample	Activ. temp. (K)	Atm.	Hydrogen donor (Glyc:donor)	TONo (10^{-3} mol_{glyc} g^{-1}_{catal} h^{-1})	Glyc. conv. (%)	Selectivity (%)			
						Acetol	1,2-PDO	Cracked[a]	Rest[b]
$Cu/Al_2O_3^{(S)}$	593	H_2	–	0.7	32.9	0.1	90.1	9.8	0.0
		N_2	2-PO (1:1)	1.5	14.6	47.5	40.5	6.1	5.9
$Ni/Al_2O_3^{(S)}$	593	H_2	–	0.5	5.2	7.2	73.7	10.5	8.4
		N_2	2-PO (1:1)	0.1	2.0	60.3	7.5	8.6	22.3
$Ni—Cu/Al_2O_3^{(S)}$	593	H_2	–	1.0	31.0	0.9	84.7	6.7	7.7
		N_2	2-PO (1:1)	4.3	41.2	41.7	48.3	5.6	4.4
$Cu/Al_2O_3^{(S)}$	723	H_2	–	2.0	57.0	0.8	72.8	20.0	6.4
		N_2	2-PO (1:1)	5.4	39.1	26.3	59.4	9.1	5.3
$Ni/Al_2O_3^{(S)}$	723	H_2	–	4.0	69.0	0.9	61.3	31.6	6.2
		N_2	2-PO (1:1)	5.6	31.8	32.6	50.4	12.3	4.7
$Ni—Cu/Al_2O_3^{(S)}$	723	H_2	–	6.1	70.5	0.6	66.9	30.1	2.4
		N_2	2-PO (1:1)	7.3	57.3	27.0	62.1	8.3	2.6
		N_2	2-PO (1:1.5)	3.6	60.4	17.6	64.6	12.6	5.1

[a] Ethane, ethylene glycol, methane and CO_2.
[b] 1,3-PDO and 1-Propanol.

Nevertheless, it can be addressed that both catalysts have similar Ni content but $Ni—Cu/Al_2O_3^{(S)}$ was prepared to reach a significant higher copper content, and hence higher MSA, as compared to $Ni—Cu/Al_2O_3^{(A)}$. Bienholz et al. have recently observed a linear relationship between copper MSA and glycerol conversion in liquid-phase glycerol hydrogenolysis [35]. Therefore, the higher glycerol conversion achieved with $Ni—Cu/Al_2O_3^{(S)}$ can be related to its higher MSA.

The time evolution of glycerol conversion for the activity tests with 723 K pre-treatment is shown in Fig. 5. Higher initial reaction rates were observed for all three catalysts in the activity tests under N_2 pressure and 2-PO compared to the activity tests under H_2 pressure (see Fig. 5A–C and Initial Turnover Number, TON_0, from Table 5). Nevertheless, the glycerol reaction rate under N_2 atmosphere decreased faster over reaction time and the final glycerol conversion values reached were higher for the tests under H_2 atmosphere. As observed in Fig. 5C and in Table 5, when the 2-PO/glycerol ratio was increased to 1.5 glycerol, Initial TON_0 values significantly decreased (from 7.3×10^{-3} to 3.6×10^{-3} mol_{glyc} $g^{-1}_{catalyst}$ h^{-1}). This finding seems to indicate that 2-PO and glycerol compete for the same active sites, and hence there must be an optimum proportion between the donor and the acceptor to enhance glycerol conversion.

The decrease in the glycerol reaction rate over reaction time in the activity tests under N_2 pressure and donor could be attributed to the fact that acetone formed through 2-PO dehydrogenation competes for active sites with glycerol or that for a high acetone concentration the 2-PO ↔ acetone + H_2 reaction could reach equilibrium and reduce the capacity of 2-PO to donor hydrogen. In order to determine the effect of the presence of acetone in glycerol conversion, another activity test was performed under N_2 atmosphere using $Ni—Cu/Al_2O_3^{(S)}$ catalyst activated at 723 K, and with 2-PO, glycerol and acetone in the feed. As observed in Fig. 5D, the initial reaction rate was not affected by the presence of acetone in the feed, with the TON_0 being 7.3×10^{-3} and 7.2×10^{-3} mol_{glyc} $g^{-1}_{catalyst}$ h^{-1} for the activity test without and with acetone, respectively. This means acetone has no inhibiting effect on the glycerol reaction rate. Concerning acetone concentration (Fig. 5D), it increased initially due to the acetone formed from 2-PO dehydrogenation, but lower acetone concentrations were measured in the next samples, indicating that under these operating conditions acetone reacted (being dehydrated to propene). Therefore, above a certain acetone concentration, acetone dehydration to propene was faster than 2-PO dehydrogenation to acetone.

Process deactivation in the activity tests under N_2 pressure plus 2-PO could also be attributed to active site deactivation. Previously

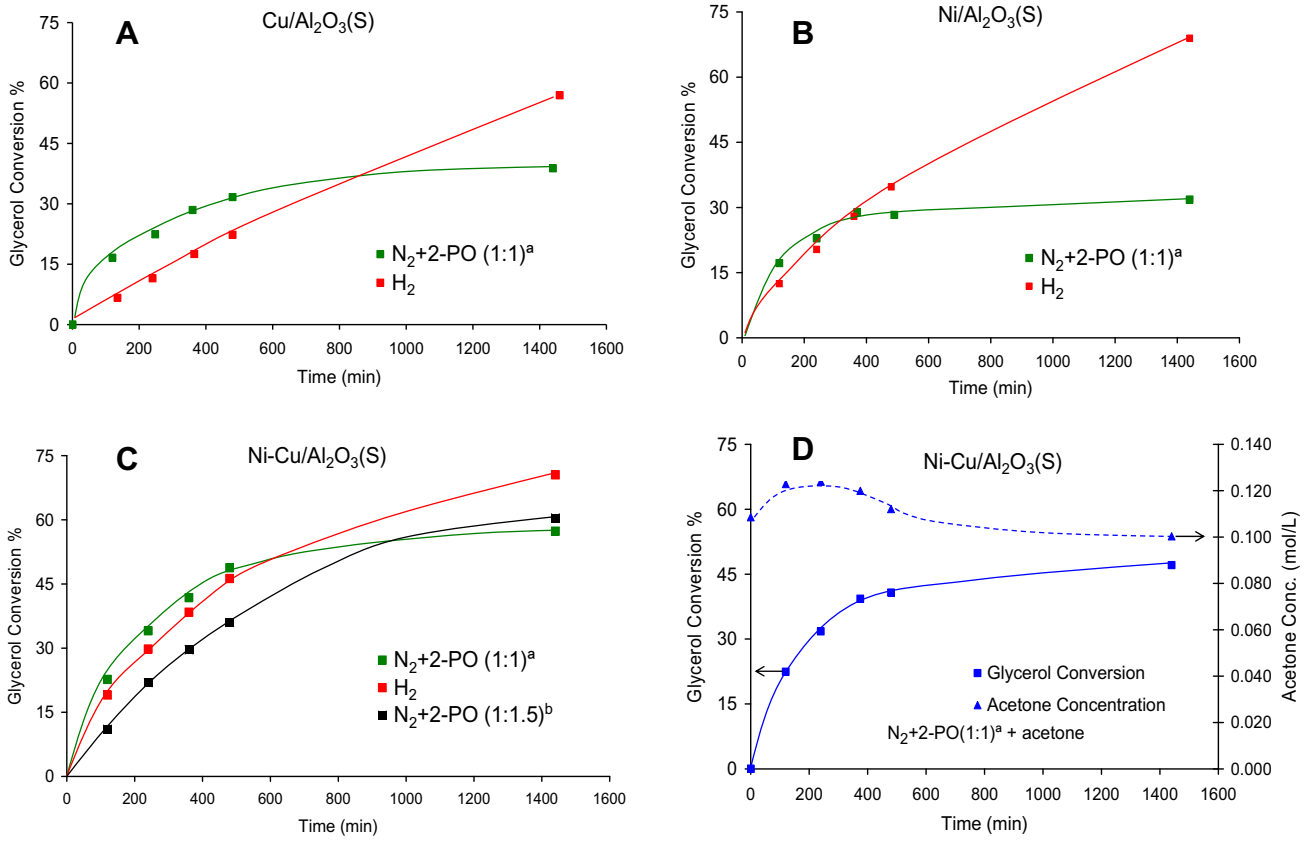

Fig. 5. Time evolution of glycerol conversion for the different catalysts and reaction atmosphere. Forty-five bar pressure, 493 K, 4 wt.% glycerol aqueous solution, 723 K activation temperature and 166 mg catalyst/g glycerol. [a](1:1 glycerol:2-PO molar ratio). [b](1:1.5 glycerol:2-PO molar ratio).

reported TGA and XPS results for spent catalyst samples showed that similar coke content and a drop in metal/Al ratios were obtained regardless of whether the process was conducted under H_2 or N_2 pressure plus hydrogen donor. However, in the process under N_2 pressure plus hydrogen donor the reaction rate decreased faster than in the process under H_2 pressure. It seems that different mechanisms/active sites are involved when the process is performed under H_2 or N_2 pressure, and that the pathway for glycerol hydrogenolysis using hydrogen from the donor is more sensitive to coke depositions than the route for glycerol hydrogenolysis using hydrogen from dissolved molecular H_2.

Table 5 summarises the selectivity values recorded in each activity test. Focusing first on the effect of the activation temperature, it is noted that the selectivity to cracked products increased when the catalysts were reduced at the higher temperature. This indicates that C–C bond cleavage is catalysed by reduced Ni and Cu sites. An analysis of the effect of the hydrogen source in the activity tests under H_2 pressure revealed very low selectivities to acetol. This means that the acetol formed from glycerol dehydration was quickly hydrogenated to 1,2-PDO and, therefore, that the reaction controlling step in glycerol hydrogenolysis under H_2 pressure was glycerol dehydration to acetol. However, under N_2 atmosphere and 2-PO, much higher selectivities to acetol were measured.

In order to study the acetol hydrogenation step, two activity tests were performed using Ni—Cu/$Al_2O_3^{(S)}$ catalyst activated at 723 K and acetol aqueous solution as the feed; the first one under H_2 pressure, and the second one under N_2 pressure and 2-PO as hydrogen source. As observed in Fig. 6, acetol reacted quickly in both activity tests. Nevertheless, in the test under H_2 pressure, most of the acetol was hydrogenated to 1,2-PDO, while under N_2 pressure and 2-PO, very low selectivity to 1,2-PDO was recorded. 2-PO conversion was slightly lower to the one obtained under the same operating conditions but with glycerol as reactant (78% and 89%, respectively). Therefore, although hydrogen species were available they could not be transferred to acetol. Moreover, in the experiments under N_2 pressure, acetol reacted to yield many different products. Identification by GC–MS revealed the formation of a wide range of C5–C6 compounds, such as 3-hexanol 5 methyl, 3-hexanone, 3,5-hexadien-2-ol. It is interesting to point out that these products were not observed in the activity tests where glycerol was the reactant, even though acetol was formed from glycerol dehydration. It seems that the competitive adsorption of acetol with glycerol and hydrogenolysis products prevents acetol from undergoing additional reactions to form C6 compounds.

At this point, two questions need to be answered: (i) the reason acetol is not hydrogenated when hydrogen comes from 2-PO and (ii) the nature of the mechanism through which glycerol is converted to 1,2-PDO when hydrogen is transferred from 2-PO.

It is well known that not all chemical species can be hydrogenated through transfer hydrogenation processes using hydrogen donors. Huang et al. proposed that transfer hydrogenation requires the consumption speed of hydrogen species in the metal sites to be quicker in the form of acceptor hydrogenation than in the form of molecular hydrogen formation and desorption [36]. When the process is conducted under N_2 pressure, hydrogen species formed from 2-PO can be transferred to an acceptor, or combine to produce H_2. When the hydrogen species are close to acetol, the formation of molecular hydrogen occurs faster than the hydrogenation of acetol, and the H_2 formed readily escapes to the gas phase. In the tests under H_2 pressure, molecular hydrogen dissolved in the aqueous phase is in equilibrium with molecular hydrogen in the gas phase. Due to the different formation pathways and adsorbtion/desorption rates, the behaviour of the hydrogen atoms formed from the

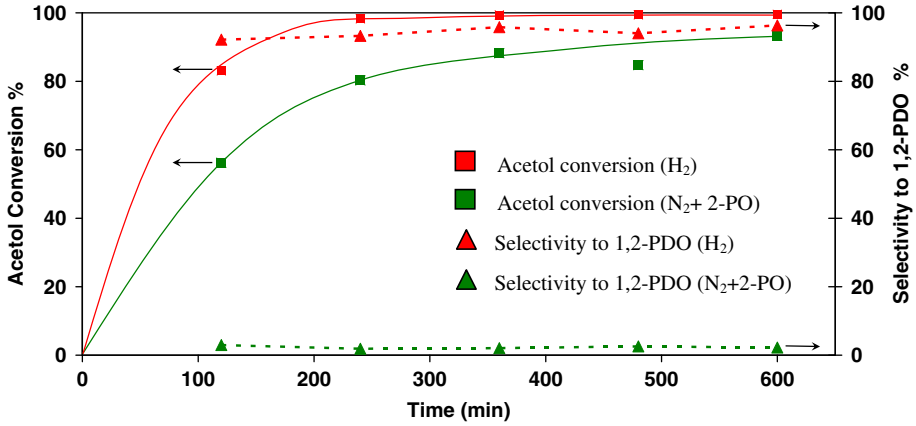

Fig. 6. Time evolution of acetol conversion and selectivity to 1,2-PDO using Ni—Cu/$Al_2O_3^{(S)}$ catalyst activated at 723 K.

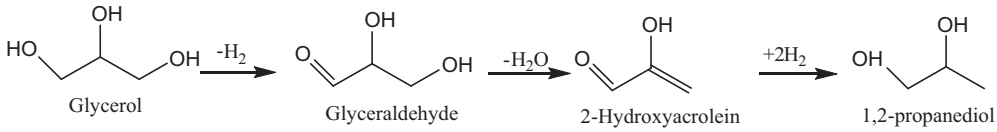

Fig. 7. Glycerol hydrogenolysis to 1,2-PDO through the glyceraldehyde pathway [37].

dissociation of dissolved molecular hydrogen differs from the behaviour of hydrogen atoms formed from 2-PO, and they are active in acetol hydrogenation.

Concerning the mechanism, Montassier et al. [37] suggested another route for the conversion of glycerol to propylene glycol under non-acid conditions. According to this mechanism, glycerol could first dehydrogenate to glyceraldehyde, followed by dehydration to 2-hydroxyacrolein and then hydrogenation to 1,2-PDO (see Fig. 7). Moreover, this route is enhanced by the addition of a base, as glyceraldehyde dehydration is supposed to be catalysed by adsorbed OH species. In order to prove whether glycerol hydrogenolysis takes place through the glyceraldehyde route when the process is conducted under N_2 pressure and 2-PO, three more activity tests were performed using Ni—Cu/$Al_2O_3^{(S)}$ catalyst. Results and operating conditions are provided in Table 6, showing that glyceraldehyde was not reactive and neither 1,2-PDO nor 2-hydroxyacrolein was detected as a reaction product. Furthermore, in the experiments where ammonia was added to increase the pH, the glycerol conversion rate decreased as compared to the tests under the same conditions but adding the base (Table 6, entries 2 and 3), indicating that acid sites have a role to play regardless of whether the process is conducted with molecular hydrogen or hydrogen donor. This is clear evidence to suggest that under the operating conditions tested glycerol hydrogenolysis did not take place through the glyceraldehyde path.

Shinmi et al. recently proposed that glycerol hydrogenolysis to 1,2-PDO under H_2 pressure and using Rh–ReO_x/SiO_2 catalyst proceeds in a single step through alkoxide adsorption [38]. We suggest that a similar mechanism occurs for glycerol hydrogenolysis using 2-PO as hydrogen donor (see Fig. 8). The first step involves alkoxide formation from 2-PO, isopropoxide, and from glycerol, 1,3-dihydroxyisopropoxide. In the second step, isopropoxide either dehydrogenates to yield acetone (Fig. 8-2A) or dehydrates to propene interacting with an acid site (Fig. 8-2B). Propene can then be hydrogenated to propane on metal sites [39] or escape to the gas phase. In the final step, the hydrogen species formed from 2-PO attacks the C–O bond of 1,3-dihydroxyisopropoxide to give 1,2-PDO (Fig. 8-3A). When there are no close hydrogen species, 1,3-dihydroxyisopropoxide can interact with an acid site and release an OH radical from the primary carbon to produce acetol [4].

Table 6
Glycerol or glyceraldehyde conversion, and yield to acetol and 1,2-PDO after 24-h reaction time. Reduction temperature 723 K, 45 bar pressure, 493 K reaction temperature, 41 mL aqueous solution and 0.27 g of catalyst.

Catalyst	Feed (mmol)	Atmos.	Initial pH	Conv %	Yield%	
					Acetol	1,2-PDO
Ni—Cu/$Al_2O_3^{(S)}$	Glyceraldehyde (13.3) 2-PO (17.8)	N_2	–	1.9	0.0	0.0
	Glycerol (17.8) 2-PO (17.8) ammonia (7.3)	N_2	11.2	26.1 (57.3)[a]	1.8 (15.4)[a]	19.2 (35.0)[a]
	Glycerol (17.8) ammonia (7.3)	H_2	11.2	17.1 (70.5)[a]	0.0 (0.4)[a]	13.8 (47.2)[a]

[a] Results obtained under the same operation conditions but without ammonia addition.

In the experiments with 2-PO as hydrogen donor, there are high amounts of hydrides coming from 2-PO, and they attack 1,3-dihydroxyisopropoxide converting it directly into 1,2-PDO. Therefore, only a small proportion of 1,3-dihydroxyisopropoxide is converted to acetol in the acid catalysed reaction. In this case, acetol remains in the media, as hydrogen species formed from 2-PO cannot hydrogenate acetol to 1,2-PDO. On the other hand, in the tests under H_2 pressure, the amount of hydrogen species adsorbed in the metal sites is lower due to the low solubility of H_2 in water solutions and they differ from hydrogen species formed from 2-PO, being less active for the direct hydrogenolysis of 1,3-dihydroxyisopropoxide. Therefore, most of the 1,3-dihydroxyisopropoxide formed is dehydrated to acetol through the acid catalysed reaction. Next, the hydrogen species from the dissolved molecular hydrogen rapidly hydrogenates the acetol formed to 1,2-PDO.

It seems that direct glycerol hydrogenolysis is more sensitive to the deactivation of the metal active sites by coke deposition as compared to the acetol pathway, due to the fact that the hydrogen donor and the acceptor must be adsorbed in adjacent sites in order

Step 1: Isopropoxide and 1,3-dihydroxyisopropoxide formation

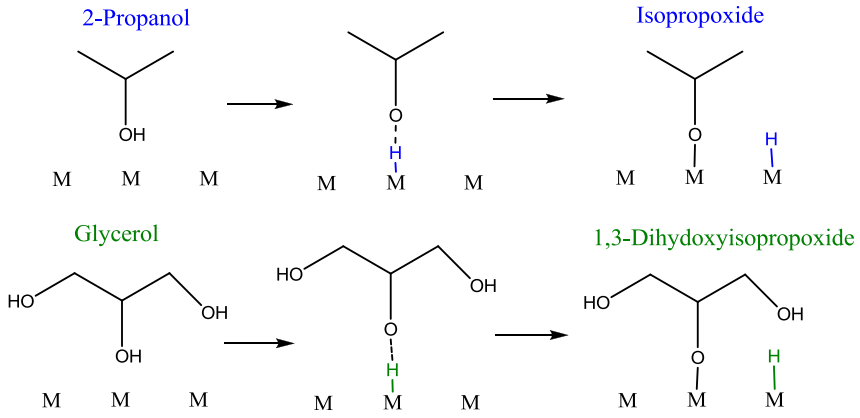

Step 2 A: Isopropoxide dehydrogenation to acetone

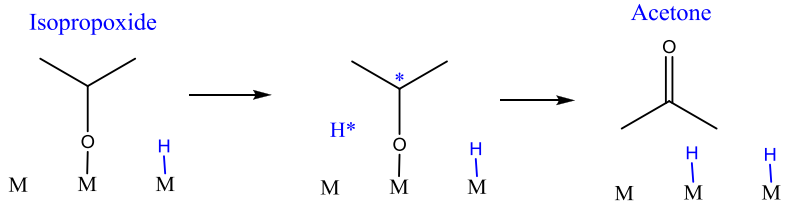

Step 2 B: Isopropoxide dehydration to propene

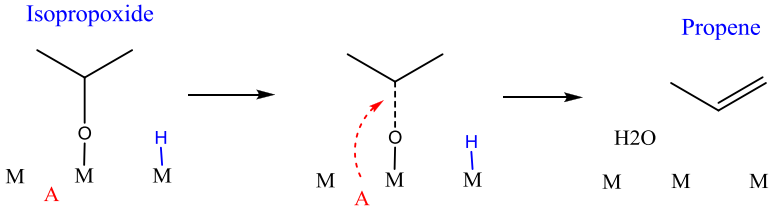

Step 3 A: 1,3-dihydroxyisopropoxide hydrogenolysis to 1,2-PDO (high atomic hydrogen concentration)

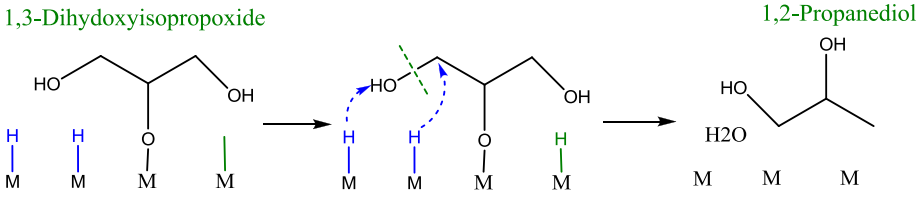

Step 3 B: 1,3-dihydroxyisopropoxide dehydration to acetol (low atomic hydrogen concentration)

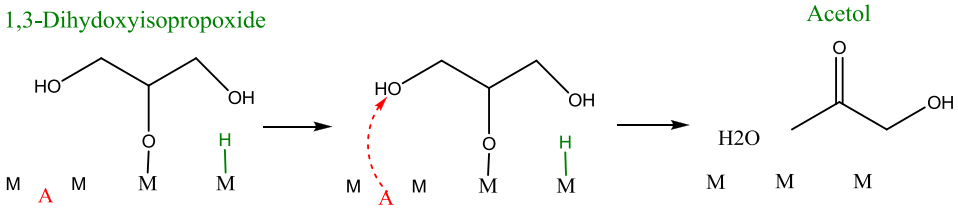

Fig. 8. Proposed reaction pathway for glycerol hydrogenolysis using 2-PO as a hydrogen donor molecule. M → Metal sites; A → Acid sites; H → hydrogen species from 2-PO; H → hydrogen species from glycerol.

to enable transfer hydrogenation. At the beginning of the process, a high amount of adjacent active sites are available in which the donor and the acceptor can adsorb and interact, but as time on stream elapses, coke formation reduces the amount of active metal sites, and the interaction between the donor and the acceptor decreases, as does the glycerol conversion rate (see Fig. 5A–C). In the process

under H_2 pressure, glycerol dehydration in the acid sites is the reaction rate controlling step, as the acetol formed readily interacts with the hydrogen species formed from molecular hydrogen, being rapidly hydrogenated in the metal sites. Hence, although the number of active metal sites is reduced with time on stream due to coke formation, there are still enough remaining ones for the fast hydrogenation of the acetol. So the decrease in metal active sites by coke deposition does not significantly affect 1,2-PDO formation through the acetol pathway.

When ammonia was added to the aqueous solution, both under N_2 and 2-PO or H_2 pressure, lower conversions were recorded. The fall was more marked in the test under H_2 pressure, which is understandable, as 1,2-PDO formation under H_2 atmosphere requires initial glycerol dehydration to acetol, where acid sites are necessary and a basic medium can deactivate them. Nevertheless, the decrease in glycerol conversion was also observed for the test under N_2 and 2-PO, with a fall in both acetol yield and 1,2-PDO yield. Hence, it seems that acid sites also have a role to play in the direct glycerol hydrogenolysis process to 1,2-PDO. Studies on CTH processes using 2-PO as hydrogen donor molecule have revealed that alkoxide formation also occurs on the alumina support [39,40]. Therefore, the addition of ammonia meant that the isopropoxide and 1,3-dihydroxy isopropoxide formation on acid sites decreased, as did 1,2-PDO formation.

The proposed mechanism also explains the reason TON_0 decreased when a higher amount of 2-PO was added to the feed: there is a competitive interaction for the metal sites between the OH group both in glycerol and in the donor. Further experiments should be conducted to obtain the optimum ratio between the donor and the acceptor in which glycerol conversion to yield 1,2-PDO is maximized.

4. Conclusions

2-Propanol proved to be more effective as a hydrogen source for the glycerol hydrogenolysis process under N_2 pressure to yield 1,2-PDO as compared to glycerol aqueous-phase reforming. The transfer hydrogenation process with 2-Propanol as hydrogen donor molecule and glycerol as acceptor was studied on Ni or/and Cu Al_2O_3 catalysts prepared by the sol–gel method. A comparison between the results of glycerol hydrogenolysis and the same operating conditions but performed under H_2 pressure suggested that different mechanisms are involved regarding the origin of the active hydrogen species. When hydrogen species come from molecular hydrogen, 1,3-dihydroxyisopropoxide is first dehydrated to acetol, which is subsequently hydrogenated to yield 1,2-propanediol. When hydrogen species come from 2-propanol dehydrogenation, 1,3-dihydroxyisopropoxide is directly converted into 1,2-propanediol and the acetol formed from 1,3-dihydroxyisopropoxide dehydration on acid sites does not react any further and remains in the media.

The glycerol reaction rate using 2-propanol as hydrogen source decreased faster with time on stream as compared to the process using molecular hydrogen. As adjacent sites are required for the donor and the acceptor for transfer hydrogenation, glycerol hydrogenolysis with 2-propanol is more sensitive to active site deactivation by coke deposition than glycerol hydrogenolysis with molecular hydrogen.

Acknowledgments

This work was supported by funds from the Spanish Ministry of Science and Innovation ENE2009-12743-C04-04, and from the Basque Government (Researcher Training Programme of the Department of Education, Universities and Research). The authors also gratefully acknowledge the University of the Basque Country and the Inorganic Chemistry Department at the University of Malaga for their technical support.

References

[1] M. Pagliaro, M. Rossi, The Future of Glycerol: New Usages for a Versatile Raw material, RSC Publishing, Cambridge, 2008.
[2] T. Miyazawa, Y. Kusunoki, K. Kunimori, K. Tomishige, J. Catal. 240 (2006) 213.
[3] M.A. Dasari, P. Kiatsimkul, W.R. Sutterlin, G.J. Suppes, Appl. Catal A: Gen. 281 (2005) 225.
[4] S. Sato, M. Akiyama, R. Takahashi, T. Hara, K. Inui, M. Yokota, Appl. Catal. A: Gen. 347 (2008) 186.
[5] M. Akiyama, S. Sato, R. Takahashi, K. Inui, M. Yokota, Appl. Catal. A: Gen. 371 (2009) 60.
[6] T. Miyazawa, S. Koso, K. Kunimori, K. Tomishige, Appl. Catal. A: Gen. 329 (2007) 30.
[7] T. Miyazawa, S. Koso, K. Kunimori, K. Tomishige, Appl. Catal. A: Gen. 318 (2007) 244.
[8] E.P. Maris, W.C. Ketchie, M. Murayama, R.J. Davis, J. Catal. 251 (2007) 281.
[9] L. Ma, D. He, Z. Li, Catal. Commun. 9 (2008) 2489.
[10] D.G. Lahr, B.H. Shanks, J. Catal. 232 (2005) 386.
[11] G.W. Huber, R.D. Cortright, J.A. Dumesic, Angew. Chem. Int. Ed. 43 (2004) 1549.
[12] R.D. Cortright, R.R. Davda, J.A. Dumesic, Nature 418 (2002) 964.
[13] E. D'Hondt, S. Van de Vyver, B.F. Sels, P.A. Jacobs, Chem. Commun. 45 (2008) 6011.
[14] I. Gandarias, P.L. Arias, J. Requies, M.B. Güemez, J.L.G. Fierro, Appl. Catal. B: Environ. 97 (2010) 248.
[15] A. Wolfson, C. Dlugy, Y. Shotland, D. Tavor, Tetrahedron Lett. 50 (2009) 5951.
[16] R.A.W. Johnstone, A.H. Wilby, I.D. Entwistle, Chem. Rev. 85 (1985) 129.
[17] M.G. Musolino, L.A. Scarpino, F. Mauriello, R. Pietropaolo, Green Chem. 11 (2009) 1511.
[18] R.A.W. Johnstone, A.H. Wilby, Tetrahedron 37 (1981) 3667.
[19] M.A. Aramendía, V. Borau, C. Jiménez, J.M. Marinas, J.R. Ruiz, F.J. Urbano, J. Mol. Catal. A: Chem. 171 (2001) 153.
[20] A.D. Dhale, L.K. Myrant, S.P. Chopade, J.E. Jackson, D.J. Miller, Chem. Eng. Sci. 59 (2004) 2881.
[21] G.M. Kramer, G.B. McVicker, J.J. Ziemiak, J. Catal. 92 (1985) 355.
[22] L. De Rogatis, T. Montini, A. Cognigni, L. Olivi, P. Fornasiero, Catal. Today 145 (2009) 176.
[23] H. Roh, K. Jun, W. Dong, J. Chang, S. Park, Y. Joe, J. Mol. Catal. A: Chem. 181 (2002) 137.
[24] M. Richter, M.J.G. Fait, R. Eckelt, E. Schreier, M. Schneider, M.-. Pohl, R. Fricke, Appl. Catal. B: Environ. 73 (2007) 269.
[25] J. Álvarez-Rodríguez, M. Cerro-Alarcón, A. Guerrero-Ruiz, I. Rodríguez-Ramos, A. Arcoya, Appl. Catal. B: Gen. 348 (2008) 241.
[26] J. Lee, E. Lee, O. Joo, K. Jung, Appl. Catal. A: Gen. 269 (2004) 1.
[27] M. Korac, Z. Andjic, M. Tasic, Z. Kamberovic, J. Serb. Chem. Soc. 72 (2007) 1115.
[28] J.-L. Li, T. Inui, Appl. Catal. A: Gen. 137 (1997) 105.
[29] J. Agrell, H. Birgersson, M. Boutonnet, I. Melián-Cabrera, R.M. Navarro, J.L.G. Fierro, J. Catal. 219 (2003) 389.
[30] X. Wang, X. Pan, R. Lin, S. Kou, W. Zou, J.-X. Ma, Int. J. Hydr. Energy 35 (2010) 4060.
[31] I. Melián-Cabrera, M.L. Granados, J.L.G. Fierro, J. Catal. 210 (2002) 285.
[32] L. Kundakovic, M. Flytzani-Stephanopoulos, Appl. Catal. A: Gen. 171 (1998) 13.
[33] A. Velon, I. Olefjord, Oxid. Metals 56 (2001) 415.
[34] A.A. Lemonidou, M.A. Goula, I.A. Vasalos, Catal. Today 46 (1998) 175.
[35] A. Bienholz, H. Hofmann, P. Claus, Appl. Catal. A: Gen. 391 (2011) 153.
[36] L. Huang, Y. Zhu, C. Huo, H. Zheng, G. Feng, C. Zhang, Y. Li, J. Mol. Catal. A: Chem. 288 (2008) 109.
[37] C. Montassier, D. Giraud, J. Barbier, Heter. Catal. Fine Chem. (1988) 165.
[38] Y. Shinmi, S. Koso, T. Kubota, Y. Nakagawa, K. Tomishige, Appl. Catal. B: Environ. 94 (2010) 318.
[39] M.I. Zaki, M.A. Hasan, L. Pasupulety, Langmuir 17 (2001) 4034.
[40] J.A. Wang, X. Bokhimi, O. Novaro, T. López, F. Tzompantzi, R. Gómez, J. Navarrete, M.E. Llanos, E. López-Salinas, J. Mol. Catal. A: Chem. 137 (1999) 239.